Diffusion Basis Spectrum Imaging of White Matter in Schizophrenia and Bipolar Disorder

Daniel Mamah*[1], Aakash Patel[1], ShingShiun Chen[1] and Yong Wang[2,3,4,5], Qing Wang*[3,4,5]

Author Affiliations:
Departments of [1]Psychiatry, [2]Obstetrics and Gynecology, [3]Mallinckrodt Institute of Radiology, and [4]Biomedical Engineering, [5]Mechanical Engineering and Materials Science
Washington University School of Medicine, St. Louis, Missouri.

Corresponding Author:
Daniel Mamah, M.D., M.P.E.
Department of Psychiatry (Campus Box 8134)
Washington University School of Medicine
660 S. Euclid
St. Louis, MO 63110
(314) 747-2160
Fax: (314) 747-2182
E-mail: mamahd@wustl.edu

Qing Wang, Ph.D.
Mallinckrodt Institute of Radiology (Campus Box 8225)
Washington University School of Medicine
4525 Scott Ave.,
Saint Louis, MO, 63110
(314)273-1344
Email: wangqing@wustl.edu

Abstract: 243 words
Text: 3,776 words
Number of tables: 2
Number of figures: 8
Number of supplementary materials: 0

Key words: Schizophrenia, bipolar disorder, neuroinflammation, diffusion, dbsi, tbss, brain, connectivity, fiber density

ABSTRACT

Background:

Multiple studies point to the role of neuroinflammation in the pathophysiology of schizophrenia (SCZ), however, there have been few *in vivo* tools for imaging brain inflammation. Diffusion basis spectrum imaging (DBSI) is an advanced diffusion-based MRI method developed to quantitatively assess microstructural alternations relating to neuroinflammation, axonal fiber, and other white matter (WM) pathologies.

Methods:

We acquired one-hour-long high-directional diffusion MRI data from young control (CON, *n* =27), schizophrenia (SCZ, *n* =21), and bipolar disorder (BPD, *n* =21) participants aged 18-30. We applied Tract-based Spatial Statistics (TBSS) to allow whole-brain WM analyses and compare DBSI-derived isotropic and anisotropic diffusion measures between groups. Clinical relationships of DBSI metrics with clinical symptoms were assessed across SCZ and control participants.

Results:

In SCZ participants, we found a generalized increase in DBSI-derived cellularity (a putative marker of neuroinflammation), a decrease in restricted fiber fraction (a putative marker of apparent axonal density), and an increase in extra-axonal water (a putative marker of vasogenic edema) across several WM tracts. There were only minimal WM abnormalities noted in BPD, mainly in regions of the corpus callosum (increase in DTI-derived RD and extra-axonal water). DBSI metrics showed significant partial correlations with psychosis and mood symptoms across groups.

Conclusion:

Our findings suggest that SCZ involves generalized white matter neuroinflammation, decreased fiber density, and demyelination, which is not seen in bipolar disorder. Larger studies are needed to identify medication-related effects. DBSI metrics could help identify high-risk groups requiring early interventions to prevent the onset of psychosis and improve outcomes.

Introduction

Schizophrenia (SCZ) is a chronically disabling psychiatric disorder afflicting 0.5-1% of the population. The pathophysiology of the disorder is unclear and complicated by the heterogeneity of clinical, postmortem, and imaging findings. However, SCZ has been associated with reductions in cortical thickness, as well as cortical surface area, primarily in frontal and temporal regions.[1] Explaining the underlying causes of cortical changes, neuropathological studies have shown increased neuronal packing density in the cortex, due to both decreased neuropil and soma size.[2] Dendrites are shorter and less branched and spine density is also lower in those with SCZ compared to healthy individuals,[3] which is thought to underlie the neuronal connectivity abnormalities reported in SCZ patients.[4] Additionally, fewer oligodendrocytes in various brain regions have been found in SCZ further contributing to neuronal dysconnectivity in the disorder, and white matter deficits found in brain imaging studies.[2]

White matter volumes are often reduced in SCZ patients, but generally to a lesser extent than cortical volumes.[5] Diffusion imaging studies in SCZ typically report lower fractional anisotropy (FA) in one or more white matter tracts, however, the specificity of significant abnormalities has been heterogeneous across studies.[6–8] The large, multi-site ENIGMA study involving 4322 individuals found widespread FA reduction in SCZ, with the anterior corona radiata (d=0.40) and corpus callosum (d=0.39) showing the greatest effects.[9] Myelin deficits are thought to play a major role in observed diffusion imaging abnormalities, considering that increased radial diffusivity is usually seen in SCZ,[10] and dysregulation of myelin-associated gene expression, reductions in oligodendrocyte numbers, and marked abnormalities in the ultrastructure of myelin sheaths have also been reported.[11]

Multiple lines of evidence have attributed neuroinflammation to SCZ,[12] which appears to precede the onset of illness.[13] Peripheral inflammatory markers (e.g., IL-1β, IL-6, and TNF-α) are often seen in individuals with SCZ,[14,15] although diagnostic specificity remains to be established and is also seen in other psychiatric disorders.[15] Robust evidence has also been reported for increased proinflammatory cytokines in the prodromal period,[16] and prenatal exposure to specific infections has

been associated with future SCZ development.[17] Furthermore, results from genetic studies support the role of immune dysregulation in the pathophysiology of SCZ – a large multi-site study found that the most significantly associated SCZ genome-wide association study (GWAS) locus lies within the major histocompatibility complex (MHC) locus on chromosome 6, which contains genes that function in the acquired immune system.[18] Finally, positron emission tomography (PET) studies done in SCZ patients, using a variety of tracers, most commonly targeting the 18 kDa translocator protein, TSPO, have shown increased binding in the disorder.[12] While PET studies can measure neuroinflammatory proteins at low concentrations, obstacles to reliable measurement remain, such as high nonspecific binding and sensitivity to a genetic polymorphism that affects the binding affinity of early TSPO radioligands.[19] Other promising neuroinflammation-targeted ligands are currently in development.[19] Outside of PET, few non-invasive alternatives for investigating neuroinflammation in the brain have been proposed.[20] In contrast to PET, such methods could facilitate longitudinal investigations, particularly in younger populations, and potentially have future clinical implications in monitoring treatment effects.

Diffusion Basis Spectrum Imaging (DBSI) is a novel multi-parametric diffusion imaging post-processing methodology that models the diffusion-weighted MRI signals as a linear combination of multiple tensors describing both the discrete anisotropic content (axonal fibers) and an isotropic diffusion spectrum component encompassing the full range of diffusivities.[21,22] DBSI acquires water diffusion signals for each imaging voxel and then uses a pattern-matching algorithm to find the minimal number of dictionary entries that best represent the acquired water diffusion signals and their relative proportions. Each identified dictionary entry represents one type of microstructure in the image voxel.[21,22] This modeling was developed to quantify intra- and extracellular water permitting the discrimination of vasogenic edema, increased cellularity, axonal injury/loss, and demyelination (see **Figure 1**).[21,22] Previous studies using DBSI have been done in Alzheimer's disease where it showed increased cellular diffusivity in both preclinical and early symptomatic phases of Alzheimer's disease consistent with white matter inflammation,[23,24] despite traditional diffusion imaging abnormalities only

identified in the symptomatic phase.[23] DBSI has also been used in multiple sclerosis,[25] cervical spondylotic myelopathy,[26] obesity,[27] and HIV,[28] but has not been used to investigate individuals with SCZ or psychosis.

Our current study investigated the brains of schizophrenia participants using the DBSI methodology. We hypothesized that due to the presumed psychopathology underlying SCZ, primary abnormalities found with this method would involve increased cellular diffusion fraction across multiple white matter tracts compared to healthy controls. In the study, we also included individuals with bipolar disorder, as an additional comparison group to establish specificity of findings. While diffusion imaging abnormalities have often been found in bipolar disorder, these are generally less extensive and severe than those seen in schizophrenia.[29] We hypothesize that similarly, cellular diffusion fraction in BPD will be increased compared to the control group but substantially less than in SCZ participants.

Methods

Subjects

Imaging data were acquired from three participant groups, aged 18 to 30-year-old recruited through community advertisements and volunteer databases: 27 healthy young control (CON), 21 schizophrenia (SCZ), and 21 bipolar disorder (BPD). These participants were diagnosed on the basis of a trained research assistant who used the Structured Clinical Interview for DSM-IV Axis I Disorders (SCID-IV).[30] CON subjects were required to have no lifetime history of psychotic or mood disorders. BPD participant patients were required to meet DSM-IV criteria for Bipolar I Disorder. To minimize clinical heterogeneity within the BPD group, only participants with a history of euphoric mania (versus mania characterized by primarily irritable mood) were included in the study. Written informed consent was obtained prior to participation, and all study protocols were approved by the Institutional Review Board at the Washington University School of Medicine in St. Louis, MO.

All participants were excluded if they: (a) met DSM-IV criteria for substance dependence or severe/moderate abuse during the prior 3 months; (b) had a clinically unstable or severe general medical disorder; or (c) had a history of head injury with documented neurological sequelae or loss of consciousness.

Behavioral assessments

Recent symptoms (i.e., in the prior two weeks) were assessed using the Scale for the Assessment of Negative Symptoms (SANS), and the Scale for the Assessment of Positive Symptoms (SAPS).[31] Chronic symptoms (i.e., prior year) were assessed using the Washington Early Recognition Center Affectivity and Psychosis (WERCAP) Screen, both affective (a-WERCAP) and psychosis (p-WERCAP) components.[32–34]

Image acquisition

Structural T1w MRI images were acquired on a 3T Siemens Prisma with a 32 channel head coil using a 3D MPRAGE sequence[35] (0.8 mm isotropic voxels, TR/TI = 2400/1000 ms, TE = 2.2 ms, flip angle = 8°**,** FOV = 256 ×240×166 mm, matrix size = 320 ×300, 208 sagittal slices, in-plane (iPAT) acceleration factor of 2). T2w volumes were also acquired at the same spatial resolution using the variable-flip-angle turbo-spin-echo 3D SPACE sequence[36] (TR/TE=3200/564 ms; same FOV, matrix and in-plane acceleration). The diffusion MRI (dMRI) scans used the multi-band (MB) sequences from the Center for Magnetic Resonance Research, with 1.25 isotropic voxels, TR = 5000 ms, TE = 104 ms, 6/8 partial Fourier, and MB factor = 4. A full dMRI session included 6 runs (each approximately 8.5 min), representing 3 different gradient tables, with each table acquired once with anterior-to-posterior and posterior-to-anterior phase encoding polarities, respectively. Each gradient table includes approximately 90 diffusion weighting directions plus 6 b = 0 acquisitions interspersed throughout each

run. Diffusion weighting consisted of 3 shells of b = 1000, 2000, and 3000 s/mm^2 interspersed with an approximately equal number of acquisitions on each shell within each run.

Image preprocessing

The diffusion data were preprocessed using the "DiffusionPreprocessing" stream of the HCPpipelines (v4.3.0),[37,38] using the QuNex container (v0.91.11). This pipeline includes intensity normalization, susceptibility distortion correction (via FSL's 'topup'),[39] and correction for eddy current distortions and motion via FSL's 'eddy' tool.[40] We used the advanced 'eddy' features of outlier replacement,[41] slice-to-volume motion correction,[42] and correction for susceptibility-by-movement interactions.[43] The b-vectors were rotated to account for motion.[44] Finally, the dMRI data was corrected for gradient nonlinearity distortion as part of resampling to the subject's native T1w space from the HCP structural pipeline output (while maintaining the same 1.25 mm spatial resolution of the dMRI data). Following that preprocessing, two different diffusion models were implemented 1) diffusion tensor estimation using conventional FSL's 'DTI' toolbox 2) modelled diffusion signal using DBSI and derived parameters such as cellular diffusion fraction, extra-axonal water, axonal fiber fraction, fiber axial, and fiber radial diffusivities. To perform voxel-wise analysis of all white matter tracts, Tract-based spatial statistics (TBSS) was used.[45] DTI-derived FA images were calculated and projected onto the mean FA skeleton, which represents center of white matter tracts, and thresholded at 0.2. After pre-alignment and skeletonization stage, the resulting 4D data was used to perform voxel-wise statistics.

DBSI

Diffusion data were modeled using the novel DBSI method. In DBSI, each of the potential pathological components, including inflammatory cell components, extra-cellular water/vasogenic edema, axonal injury/loss, and demyelination, is modelled within each voxel by a dedicated diffusion tensor. DBSI framework, as shown in Equation (1), considers diffusion-weighted MRI data as a linear

combination of multiple anisotropic (crossing myelinated and unmyelinated axons of varied direction; the first term) and a spectrum of isotropic (cells, sub-cellular structure, and edematous water; the second term)[22] diffusion tensors.

$$S_k = \sum_{i=1}^{N_{Aniso}} f_i e^{-|\overrightarrow{b_k}|\cdot\lambda_{\perp\_i}} e^{-|\overrightarrow{b_k}|\cdot(\lambda_{\parallel\_i}-\lambda_{\perp\_i})\cdot cos^2\psi_{ik}} + \int_a^b f(D)e^{-|\overrightarrow{b_k}|D}dD \ (k = 1,2,\dots,K)$$

The quantities S_k and $|\overrightarrow{b_k}|$ are the signal and b-value of the k^{th} diffusion gradient, N_{Aniso} is the number of anisotropic tensors (fiber tracts), ψ_{ik} is the angle between the k^{th} diffusion gradient and the principal direction of the i^{th} anisotropic tensor, $\lambda_{\parallel\_i}$ and $\lambda_{\perp\_i}$ are the axial and radial diffusivities of the i^{th} anisotropic tensor, f_i is the signal intensity fraction for the i^{th} anisotropic tensor, and a and b are the low and high diffusivity limits for the isotropic diffusion spectrum $f(D)$. In this study, the sum of f_i is defined as the fiber fraction to reflect the total white matter axonal fiber density. The summation of the anisotropic diffusion component with radial diffusivity bigger than 0.1 ($\times 10^{-3}$ mm^2/s) is defined as the extra-axonal water fraction to reflect the extra-axonal water edema in WM. The summation of the isotropic diffusion components with apparent diffusion coefficient between 0 and 0.3 ($\times 10^{-3}$ mm^2/s) is defined as the cellular diffusion fraction to reflect the total cellularity in WM.

Statistical analysis

Statistical analysis was performed using Kruskal-Wallis rank sum test for age and body mass index (BMI), and Pearson's χ^2 test for gender. These statistical analyses were performed with the software package R, Version 4.3.1 (https://www.r-project.org/).

To perform voxel-wise group comparisons, a permutation based nonparametric statistical test was performed using "randomise" — a part of FSL.[46] Two sample non-parametric t-tests were performed between CON, BPD, and SCZ groups. The mean FA skeleton was used as mask and number of permutations were set to 5000. The significance threshold for group differences was set at $p < 0.05$. The statistical significance maps were corrected for multiple comparisons using threshold free cluster

enhancement (TFCE) option in "randomise". Similarly, group comparisons of DBSI metrics were performed.

For each DBSI measure, voxels with statistically significant difference ($p < 0.05$ after FWER correction) resulting from group wise comparisons 1) control vs schizophrenia, and 2) control vs bipolar disorder were added together, and binary mask was created. DBSI measures were summarized for each subject using corresponding mask. Finally, Pearson's correlation was performed between DBSI measures (only with statistically significant group difference in randomized test) and clinical scores with the software package R. As age and gender were not statistically different across groups, we did not control for it in above analysis.

Results

Demographic and clinical profiles:

Table 1 shows demographic and clinical information across the participant groups. Mean age was similar across the three participant groups. The BPD group had substantially more females than males, while sex was more balanced in SCZ and CON.

Voxel-wise analysis of DTI-derived fractional anisotropy, radial diffusivity, and axial diffusivity

Table 2 shows white matter tracts where DBSI and DTI measures are significantly different in schizophrenia and bipolar disorder groups compared to control group.

As shown in **Figure 2A**, we observed low fractional anisotropy (FA) in SCZ compared to controls. The reduced FA was bilaterally distributed over anterior thalamic radiation, corticospinal tract, cingulum (both cingulate gyrus and hippocampus), forceps major, forceps minor, inferior fronto-occipital fasciculus, inferior longitudinal fasciculus, and superior longitudinal fasciculus. In contrast to findings in SCZ, the FA in BPD participants were minimal and were only observed unilaterally over

anterior thalamic radiation, inferior fronto-occipital fasciculus, uncinate fasciculus, bilaterally in cingulum (cingulate gyrus) and forceps minor (**Figure 2B**).

No significant axial diffusivity (AD) abnormalities were seen in either SCZ (**Figure 2C**) or BPD (**Figure 2D**) participants. SCZ subjects however had significantly higher radial diffusivity (RD) than controls in similar regions where decreased FA was observed, as shown in **Figure 2E**. No significant abnormalities in RD were observed in BPD (**Figure 2F**).

Voxel-wise analysis of cellular diffusion fraction

Relative to controls, SCZ had significantly increased cellular diffusion fraction — a putative marker of white matter inflammation (**Figure 3**A), bilaterally spread over anterior thalamic radiation, corticospinal tract, cingulum bundle, forceps major, forceps minor, inferior fronto-occipital fasciculus, uncinate fasciculus, and superior longitudinal fasciculus.

No significant alterations in cellular diffusion fraction were observed in BPD after FWER correction (**Figure 3**B).

Voxel-wise analysis of axonal fiber fraction

Compared to controls, SCZ had statistically decreased fiber fraction (**Figure 4**A) bilaterally in anterior thalamic radiation, corticospinal tract, cingulum bundle, forceps major, forceps minor, inferior fronto-occipital fasciculus, uncinate fasciculus, and temporal region of superior longitudinal fasciculus.

Compared to controls, changes in the axonal fiber fraction were not statistically significant in BPD (**Figure 4**B).

Voxel-wise analysis of extra-axonal water fraction

As shown in **Figure 5**, compared to controls, SCZ and BPD had statistically increased extra-axonal water fraction (Panel A and Panel B respectively). In both SCZ and BPD, increased extra-axonal

water fraction was present bilaterally over anterior thalamic radiation, corticospinal tract, cingulum bundle, forceps major, forceps minor, inferior fronto-occipital fasciculus, inferior longitudinal fasciculus, uncinate fasciculus, and superior longitudinal fasciculus.

Group comparison between SCZ and BPD did not reveal significant differences in the extra-axonal water fraction.

Voxel-wise analysis of DBSI-derived fiber axial and fiber radial diffusivity

Compared to controls, fiber axial diffusivity changes in SCZ (**Figure 6**A), and BPD (**Figure 6**B) did not survive the significance threshold after FWER correction.

Relative to controls, SCZ (**Figure 6**C) had significantly increased fiber radial diffusivity, spread bilaterally over anterior thalamic radiation, corticospinal tract, cingulum bundle, forceps major, forceps minor, inferior fronto-occipital fasciculus, inferior longitudinal fasciculus, uncinate fasciculus, and superior longitudinal fasciculus. In BPD (**Figure 6**D), increased fiber radial diffusivity was observed bilaterally over anterior thalamic radiation, corticospinal tract, cingulum bundle, forceps major, forceps minor, inferior fronto-occipital fasciculus, superior longitudinal fasciculus, unilaterally in right inferior longitudinal fasciculus and left uncinate fasciculus.

Correlation analysis between WERCAP symptom score and DBSI measures

Across healthy control and SCZ, a correlation of psychotic symptom scores against DBSI measures partialled for diagnosis showed significant effects ($r>0.55$; $p<0.0001$) for cellular diffusion fraction (**Figure 7A**), fiber radial diffusivity (**Figure 7B**), fiber fraction (**Figure 7C**) and extra-axonal

water fraction (**Figure 7D**). The relationship between psychotic symptoms and DBSI metrics separately in SCZ and control participants did not meet statistical significance.

Similar findings were observed for the relationship between mood symptom scores and DBSI measures (**Figures 8A-D**), though the relationship was weaker ($r>0.28$; $p<0.05$).

Discussion

Our study expands the novel neuroimaging, diffusion basis spectrum imaging (DBSI), for the first time to the study of individuals with schizophrenia and bipolar disorder. DBSI is particularly promising in the study of those with psychiatric disorders, which generally do not have validated biomarkers with clinical utility. This method has been shown to distinguish various pathophysiologic changes of brain white matter in vivo in postmortem studies of central nervous system disorders.[47]

The commonly used diffusion imaging metrics DTI-derived FA, RD and AD have been valuable in understanding brain microstructural abnormality in disease. However, establishing underlying when these metrics are abnormal is complicated by the fact that different pathologies can contribute to it. For example, while high RD is suggested to be largely related to axonal demyelination, other factors like edema and cellularity can confound symptoms. By delineating individual white matter components, DBSI-derived RD and AD are posited to minimize confounding effects, compared to DTI-derived metrics. Our study found a generalized bilateral increase in white matter RD in schizophrenia, without associated abnormality in AD. This suggests that demyelination and not axonal degeneration is likely the underlying microstructural pathology.[48] A minimally elevated RD was also seen in BPD participants but only with DBSI, not with conventional DTI. Demyelination of white matter tracts is consistent with previous studies of schizophrenia. Postmortem samples have shown oligodendrocytes have been found to show consistent signs of dystrophia, apoptosis and/or necrosis, and their numerical density have been significantly reduced in schizophrenia.[49] Schizophrenia brain samples have also been characterized by downregulation of myelin-specific structural proteins and a reduction in mRNA levels of

oligodendroglial lineage transcription factors, such as OLIG1, OLIG2 and SOX10.[50] Myelin-related abnormalities in schizophrenia would lead to disconnection of neural networks by impairing the saltatory conduction and information conduction between neurons.[51] Findings of high RD in schizophrenia appear to be disorder-specific, as similar changes were seen to a milder degree, consistent with fewer white matter abnormalities found in other studies.[52]

A notable finding in our study was an elevated cellular diffusion fraction across multiple white matter regions exclusively in schizophrenia subjects. The DBSI metric generally correlates with elevated inflammatory cells and is seen in brain conditions with inflammatory underpinnings, such as multiple sclerosis,[22] HIV infection,[28] and autoimmune encephalitis in mice.[53] There has been increasing evidence for an inflammatory signature in the brain in schizophrenia, including overexpression of pro-inflammatory cytokines,[54] changes to the blood-brain barrier with macrophage infiltration[55] and possible microglia activation.[56] Schizophrenia has also been associated with elevated peripheral inflammatory markers,[14,15] binding of pro-inflammatory PET tracers,[12] and genetic risk factors of immune dysregulation.[18] Inflammatory markers have been found to precede the onset of illness[13,16] suggesting a progressive pathological process leading to an onset of schizophrenia. The absence of cellular diffusion fraction abnormalities in our bipolar disorder population suggests the specificity of this DBSI marker to schizophrenia. Although not clear from our results, it is worth speculating whether increased cellular diffusion fraction is confounded by increased density of interstitial white matter neurons in schizophrenia,[57] reflecting a deficiency in interneuron migration from white matter to cortex during development. Migration of these subplate neurons has been associated with environmental insults including maternal infection in early life and cannabis use during childhood and adolescence.[58]

Another major finding in our study involved a decreased fiber fraction in schizophrenia participants, a marker of apparent axonal fiber density. Here again, findings were bilateral and generalized to multiple white matter tracts throughout the brain. There have been few studies investigating white matter fiber density in schizophrenia, however, results have been somewhat

consistent. A 'fixel-based' analysis of diffusion imaging data indicated lower primary fiber density in the postcentral and posterior corpus callosum in schizophrenia patients,[59] although with higher associated fiber density in secondary and tertiary fibers. A diffusion imaging study of first-episode psychosis using NODDI analysis found decreased neurite density in multiple white matter tracts bilaterally or on the left[60] suggesting these changes occur early in the course of illness. Aberrant white matter neurodevelopment is likely to precede the onset of schizophrenia, suggesting structural vulnerability to the disorder.[61] Reduced fiber density might arise from aberrant neuronal migration, axon guidance, or synaptic pruning,[62] and underlie much of the dysconnectivity characteristic of the disorder. Future longitudinal studies of fiber density in those at clinical high risk for psychosis (CHR-P) using DBSI would provide further insights into changes in white matter structure with psychosis progression. In contrast to fiber density, it is notable that postmortem studies of neuronal density in schizophrenia have been mixed, with most postmortem studies reporting both increased[63] and decreased[59] neuronal density in schizophrenia, along with decreased dendritic spine density[64] believed to underlie altered synaptic connectivity and clinical presentation of schizophrenia patients.

Along with increased cellular diffusion fraction and decreased fiber fraction, we also found elevated extra-axonal water fraction, a marker of extra-axonal water edema, across multiple white matter tracts in schizophrenia participants. Taken together, these findings suggest that in our schizophrenia patients, there exists a pattern of inflammatory demyelination of low-density fiber tracts, with associated extra-axonal water edema. In bipolar disorder, microstructural changes suggested by DBSI results were milder degrees of demyelination and extra-axonal water edema only. Our findings also suggest that increased cellularity and decreased fiber density were specific to schizophrenia participants and may thus represent a disorder-specific biomarker representing a more extensive dysconnectivity syndrome.

More importantly, it suggests that schizophrenia involves aberrant neurodevelopment of white matter tracts.

There are some limitations to our study. Due to the relatively small sample size, we did not control for potential confounders such as medications and substance use which are more common in those with severe psychiatric illnesses than in healthy controls. Antipsychotic medications for example have been associated with reductions in white matter FA[65] and increases in white matter volume.[66] Similarly, earlier age of first cannabis use has been linked to decreased FA and increased RD in long-range tracts.[67] Thus, some of the white matter abnormalities observed in this study may be related to above factors, requiring larger studies to investigate. However, the absence of substantial findings in those with bipolar disorder, which has among the highest rates of substance use may partly argue against a major role in our findings,[68] patterns of substance use tend to differ between disorders, with schizophrenia subjects more likely using non-alcoholic drugs.[68] Secondly, while DBSI has been validated in preclinical models of white matter injury[69] and in autopsied multiple sclerosis brain specimens,[70] these results may not be completely valid in schizophrenia patients. A validation study involving postmortem schizophrenia samples is currently ongoing by our group. Thirdly, while the characteristic DBSI findings reported were observed in the majority of schizophrenia participants, they were not present in several participants, consistent with the heterogeneous brain profiles of the disorder.[7] Larger sample sizes and longitudinal investigations would provide deeper insight into distinct schizophrenia biotypes, and brain changes at varying time points across the life span.

Our study shows that a novel diffusion imaging method, DBSI, could be used to safely identify unique microstructural changes in the brain, and has potential for clinical application in the future, including personalizing therapies. Specific white matter structural abnormalities, such as decreased neurite density, likely relate to poorer long-term prognosis and response to specific medications,[60] and can therefore aid in the treatment selection. DBSI metrics could be used to monitor treatment effects,

and may also identify individuals most at risk for developing psychosis who would benefit from preventative interventions before the onset of psychosis.

Acknowledgments and Disclosures:

This work was supported by the National Institute of Mental Health (Grant No. R01MH104414 [to DM]; and Grant No. R21MH131962 [to DM and YW];). All authors report no biomedical financial interests or potential conflicts of interest.

References:

1. Godwin D, Alpert KI, Wang L, Mamah D. Regional cortical thinning in young adults with schizophrenia but not psychotic or non-psychotic bipolar I disorder. *Int J Bipolar Disord*. 2018;6(1):16. doi:10.1186/s40345-018-0124-x
2. Jaaro-Peled H, Ayhan Y, Pletnikov M V., Sawa A. Review of Pathological Hallmarks of Schizophrenia: Comparison of Genetic Models With Patients and Nongenetic Models. *Schizophr Bull*. 2010;36(2):301-313. doi:10.1093/schbul/sbp133
3. BYNE W, KIDKARDNEE S, TATUSOV A, YIANNOULOS G, BUCHSBAUM M, HAROUTUNIAN V. Schizophrenia-associated reduction of neuronal and oligodendrocyte numbers in the anterior principal thalamic nucleus. *Schizophr Res*. 2006;85(1-3):245-253. doi:10.1016/j.schres.2006.03.029
4. Black JE, Kodish IM, Grossman AW, et al. Pathology of Layer V Pyramidal Neurons in the Prefrontal Cortex of Patients With Schizophrenia. *American Journal of Psychiatry*. 2004;161(4):742-744. doi:10.1176/appi.ajp.161.4.742
5. Kubicki M, McCarley RW, Shenton ME. Evidence for white matter abnormalities in schizophrenia. *Curr Opin Psychiatry*. 2005;18(2):121-134. doi:10.1097/00001504-200503000-00004
6. Mamah D, Ji A, Rutlin J, Shimony JS. White matter integrity in schizophrenia and bipolar disorder: Tract- and voxel-based analyses of diffusion data from the Connectom scanner. *Neuroimage Clin*. 2019;21:101649. doi:10.1016/j.nicl.2018.101649
7. Arnedo J, Mamah D, Baranger DA, et al. Decomposition of brain diffusion imaging data uncovers latent schizophrenias with distinct patterns of white matter anisotropy. *Neuroimage*. 2015;120:43-54. doi:10.1016/j.neuroimage.2015.06.083

8. Mamah D, Conturo TE, Harms MP, et al. Anterior thalamic radiation integrity in schizophrenia: A diffusion-tensor imaging study. *Psychiatry Res Neuroimaging*. 2010;183(2):144-150. doi:10.1016/j.pscychresns.2010.04.013
9. Kelly S, Jahanshad N, Zalesky A, et al. Widespread white matter microstructural differences in schizophrenia across 4322 individuals: results from the ENIGMA Schizophrenia DTI Working Group. *Mol Psychiatry*. 2018;23(5):1261-1269. doi:10.1038/mp.2017.170
10. Levitt JJ, Alvarado JL, Nestor PG, et al. Fractional anisotropy and radial diffusivity: Diffusion measures of white matter abnormalities in the anterior limb of the internal capsule in schizophrenia. *Schizophr Res*. 2012;136(1-3):55-62. doi:10.1016/J.SCHRES.2011.09.009
11. Alba-Ferrara LM, de Erausquin GA. What does anisotropy measure? Insights from increased and decreased anisotropy in selective fiber tracts in schizophrenia. *Front Integr Neurosci*. 2013;7. doi:10.3389/fnint.2013.00009
12. Marques TR, Ashok AH, Pillinger T, et al. Neuroinflammation in schizophrenia: meta-analysis of *in vivo* microglial imaging studies. *Psychol Med*. 2019;49(13):2186-2196. doi:10.1017/S0033291718003057
13. Khoury R, Nasrallah HA. Inflammatory biomarkers in individuals at clinical high risk for psychosis (CHR-P): State or trait? *Schizophr Res*. 2018;199:31-38. doi:10.1016/j.schres.2018.04.017
14. Goldsmith DR, Rapaport MH, Miller BJ. A meta-analysis of blood cytokine network alterations in psychiatric patients: comparisons between schizophrenia, bipolar disorder and depression. *Mol Psychiatry*. 2016;21(12):1696-1709. doi:10.1038/mp.2016.3
15. Bishop JR, Zhang L, Lizano P. Inflammation Subtypes and Translating Inflammation-Related Genetic Findings in Schizophrenia and Related Psychoses: A Perspective on Pathways for Treatment Stratification and Novel Therapies. *Harv Rev Psychiatry*. 2022;30(1):59-70. doi:10.1097/HRP.0000000000000321
16. Corsi-Zuelli F, Deakin B. Impaired regulatory T cell control of astroglial overdrive and microglial pruning in schizophrenia. *Neurosci Biobehav Rev*. 2021;125:637-653. doi:10.1016/j.neubiorev.2021.03.004
17. Brown AS, Derkits EJ. Prenatal Infection and Schizophrenia: A Review of Epidemiologic and Translational Studies. *American Journal of Psychiatry*. 2010;167(3):261-280. doi:10.1176/appi.ajp.2009.09030361
18. Ruzzo EK, Geschwind DH. Schizophrenia genetics complements its mechanistic understanding. *Nat Neurosci*. 2016;19(4):523-525. doi:10.1038/nn.4277
19. Narayanaswami V, Dahl K, Bernard-Gauthier V, Josephson L, Cumming P, Vasdev N. Emerging PET Radiotracers and Targets for Imaging of Neuroinflammation in Neurodegenerative Diseases: Outlook Beyond TSPO. *Mol Imaging*. 2018;17:153601211879231. doi:10.1177/1536012118792317
20. Quarantelli M. MRI/MRS in neuroinflammation: methodology and applications. *Clin Transl Imaging*. 2015;3(6):475-489. doi:10.1007/s40336-015-0142-y
21. Wang Y, Sun P, Wang Q, et al. Differentiation and quantification of inflammation, demyelination and axon injury or loss in multiple sclerosis. *Brain*. 2015;138(5):1223-1238. doi:10.1093/brain/awv046
22. Wang Y, Wang Q, Haldar JP, et al. Quantification of increased cellularity during inflammatory demyelination. *Brain*. 2011;134(12):3590-3601. doi:10.1093/brain/awr307
23. Wang Q, Wang Y, Liu J, et al. Quantification of white matter cellularity and damage in preclinical and early symptomatic Alzheimer's disease. *Neuroimage Clin*. 2019;22:101767. doi:10.1016/j.nicl.2019.101767

24. Wu W, Wang Q, Sun Z, et al. Initial Correlation Analysis of Diffusion Basis Spectrum Imaging of Alzheimer's Brain and Quantitative Histology. *Alzheimer's & Dementia*. 2022;18(S6). doi:10.1002/alz.064265
25. Cross AH, Song SK. "A new imaging modality to non-invasively assess multiple sclerosis pathology." *J Neuroimmunol*. 2017;304:81-85. doi:10.1016/j.jneuroim.2016.10.002
26. Zhang JK, Sun P, Jayasekera D, et al. Utility of Diffusion Basis Spectrum Imaging in Quantifying Baseline Disease Severity and Prognosis of Cervical Spondylotic Myelopathy. *Spine (Phila Pa 1976)*. 2022;47(24):1687-1693. doi:10.1097/BRS.0000000000004456
27. Samara A, Murphy T, Strain J, et al. Neuroinflammation and White Matter Alterations in Obesity Assessed by Diffusion Basis Spectrum Imaging. *Front Hum Neurosci*. 2020;13. doi:10.3389/fnhum.2019.00464
28. Strain JF, Burdo TH, Song SK, et al. Diffusion Basis Spectral Imaging Detects Ongoing Brain Inflammation in Virologically Well-Controlled HIV+ Patients. *JAIDS Journal of Acquired Immune Deficiency Syndromes*. 2017;76(4):423-430. doi:10.1097/QAI.0000000000001513
29. Nortje G, Stein DJ, Radua J, Mataix-Cols D, Horn N. Systematic review and voxel-based meta-analysis of diffusion tensor imaging studies in bipolar disorder. *J Affect Disord*. 2013;150(2):192-200. doi:10.1016/j.jad.2013.05.034
30. First M, Spitzer R, Gibbon M, Williams B. Structured clinical interview for DSM-IV axis I disorders, clinical version (SCID-CV). In: American Psychiatric Publishing; 1996.
31. Andreasen NC. Methods for assessing positive and negative symptoms. *Mod Probl Pharmacopsychiatry*. 1990;24:73-88. doi:10.1159/000418013
32. Mamah D, Mutiso VN, Ndetei DM. Psychotic-like experiences among 9,564 Kenyan adolescents and young adults. *Psychiatry Res*. 2021;302:113994. doi:10.1016/j.psychres.2021.113994
33. Mamah D, Mutiso VN, Ndetei DM. Longitudinal and cross-sectional validation of the WERCAP screen for assessing psychosis risk and conversion. *Schizophr Res*. 2022;241:201-209. doi:10.1016/j.schres.2022.01.031
34. Mamah D, Owoso A, Sheffield JM, Bayer C. The WERCAP Screen and the WERC Stress Screen: psychometrics of self-rated instruments for assessing bipolar and psychotic disorder risk and perceived stress burden. *Compr Psychiatry*. 2014;55(7):1757-1771. doi:10.1016/j.comppsych.2014.07.004
35. Mugler JP, Brookeman JR. Three-dimensional magnetization-prepared rapid gradient-echo imaging (3D MP RAGE). *Magn Reson Med*. 1990;15(1):152-157. doi:10.1002/mrm.1910150117
36. Mugler JP, Bao S, Mulkern R V., et al. Optimized Single-Slab Three-dimensional Spin-Echo MR Imaging of the Brain. *Radiology*. 2000;216(3):891-899. doi:10.1148/radiology.216.3.r00au46891
37. Glasser MF, Sotiropoulos SN, Wilson JA, et al. The minimal preprocessing pipelines for the Human Connectome Project. *Neuroimage*. 2013;80:105-124. doi:10.1016/j.neuroimage.2013.04.127
38. Glasser MF, Smith SM, Marcus DS, et al. The Human Connectome Project's neuroimaging approach. *Nat Neurosci*. 2016;19(9):1175-1187. doi:10.1038/nn.4361
39. Andersson JLR, Skare S, Ashburner J. How to correct susceptibility distortions in spin-echo echo-planar images: application to diffusion tensor imaging. *Neuroimage*. 2003;20(2):870-888. doi:10.1016/S1053-8119(03)00336-7
40. Andersson JLR, Sotiropoulos SN. An integrated approach to correction for off-resonance effects and subject movement in diffusion MR imaging. *Neuroimage*. 2016;125:1063-1078. doi:10.1016/j.neuroimage.2015.10.019
41. Andersson JLR, Graham MS, Zsoldos E, Sotiropoulos SN. Incorporating outlier detection and replacement into a non-parametric framework for movement and distortion correction of diffusion MR images. *Neuroimage*. 2016;141:556-572. doi:10.1016/j.neuroimage.2016.06.058

42. Andersson JLR, Graham MS, Drobnjak I, Zhang H, Filippini N, Bastiani M. Towards a comprehensive framework for movement and distortion correction of diffusion MR images: Within volume movement. *Neuroimage*. 2017;152:450-466. doi:10.1016/j.neuroimage.2017.02.085
43. Andersson JLR, Graham MS, Drobnjak I, Zhang H, Campbell J. Susceptibility-induced distortion that varies due to motion: Correction in diffusion MR without acquiring additional data. *Neuroimage*. 2018;171:277-295. doi:10.1016/j.neuroimage.2017.12.040
44. Sotiropoulos SN, Jbabdi S, Xu J, et al. Advances in diffusion MRI acquisition and processing in the Human Connectome Project. *Neuroimage*. 2013;80:125-143. doi:10.1016/j.neuroimage.2013.05.057
45. Smith SM, Jenkinson M, Johansen-Berg H, et al. Tract-based spatial statistics: voxelwise analysis of multi-subject diffusion data. *Neuroimage*. 2006;31(4):1487-1505. doi:10.1016/j.neuroimage.2006.02.024
46. Winkler AM, Ridgway GR, Webster MA, Smith SM, Nichols TE. Permutation inference for the general linear model. *Neuroimage*. 2014;92:381-397. doi:https://doi.org/10.1016/j.neuroimage.2014.01.060
47. Chiang CW, Wang Y, Sun P, et al. Quantifying white matter tract diffusion parameters in the presence of increased extra-fiber cellularity and vasogenic edema. *Neuroimage*. 2014;101:310-319. doi:10.1016/j.neuroimage.2014.06.064
48. Baijot J, Van Laethem D, Denissen S, et al. Radial diffusivity reflects general decline rather than specific cognitive deterioration in multiple sclerosis. *Sci Rep*. 2022;12(1):21771. doi:10.1038/s41598-022-26204-z
49. Vostrikov VM, Uranova NA. Reduced density of oligodendrocytes and oligodendrocyte clusters in the caudate nucleus in major psychiatric illnesses. *Schizophr Res*. 2020;215:211-216. doi:10.1016/j.schres.2019.10.027
50. Tkachev D, Mimmack ML, Ryan MM, et al. Oligodendrocyte dysfunction in schizophrenia and bipolar disorder. *The Lancet*. 2003;362(9386):798-805. doi:10.1016/S0140-6736(03)14289-4
51. Roussos P, Haroutunian V. Schizophrenia: susceptibility genes and oligodendroglial and myelin related abnormalities. *Front Cell Neurosci*. 2014;8. doi:10.3389/fncel.2014.00005
52. Mamah D, Chen S, Shimony JS, Harms MP. Tract-based analyses of white matter in schizophrenia, bipolar disorder, aging, and dementia using high spatial and directional resolution diffusion imaging: a pilot study. *Front Psychiatry*. 2024;15. https://www.frontiersin.org/journals/psychiatry/articles/10.3389/fpsyt.2024.1240502
53. Wang X, Cusick MF, Wang Y, et al. Diffusion basis spectrum imaging detects and distinguishes coexisting subclinical inflammation, demyelination and axonal injury in experimental autoimmune encephalomyelitis mice. *NMR Biomed*. 2014;27(7):843-852. doi:10.1002/nbm.3129
54. Fillman SG, Sinclair D, Fung SJ, Webster MJ, Shannon Weickert C. Markers of inflammation and stress distinguish subsets of individuals with schizophrenia and bipolar disorder. *Transl Psychiatry*. 2014;4(2):e365-e365. doi:10.1038/tp.2014.8
55. Cai HQ, Catts VS, Webster MJ, et al. Increased macrophages and changed brain endothelial cell gene expression in the frontal cortex of people with schizophrenia displaying inflammation. *Mol Psychiatry*. 2020;25(4):761-775. doi:10.1038/s41380-018-0235-x
56. Howes OD, McCutcheon R. Inflammation and the neural diathesis-stress hypothesis of schizophrenia: a reconceptualization. *Transl Psychiatry*. 2017;7(2):e1024-e1024. doi:10.1038/tp.2016.278
57. Yang Y, Fung SJ, Rothwell A, Tianmei S, Weickert CS. Increased Interstitial White Matter Neuron Density in the Dorsolateral Prefrontal Cortex of People with Schizophrenia. *Biol Psychiatry*. 2011;69(1):63-70. doi:10.1016/j.biopsych.2010.08.020

58. Duchatel RJ, Shannon Weickert C, Tooney PA. White matter neuron biology and neuropathology in schizophrenia. *NPJ Schizophr*. 2019;5(1):10. doi:10.1038/s41537-019-0078-8
59. Grazioplene RG, Bearden CE, Subotnik KL, et al. Connectivity-enhanced diffusion analysis reveals white matter density disruptions in first episode and chronic schizophrenia. *Neuroimage Clin*. 2018;18:608-616. doi:10.1016/j.nicl.2018.02.015
60. Rae CL, Davies G, Garfinkel SN, et al. Deficits in Neurite Density Underlie White Matter Structure Abnormalities in First-Episode Psychosis. *Biol Psychiatry*. 2017;82(10):716-725. doi:10.1016/j.biopsych.2017.02.008
61. Canu E, Agosta F, Filippi M. A selective review of structural connectivity abnormalities of schizophrenic patients at different stages of the disease. *Schizophr Res*. 2015;161(1):19-28. doi:10.1016/j.schres.2014.05.020
62. Sellgren CM, Gracias J, Watmuff B, et al. Increased synapse elimination by microglia in schizophrenia patient-derived models of synaptic pruning. *Nat Neurosci*. 2019;22(3):374-385. doi:10.1038/s41593-018-0334-7
63. Selemon LD, Rajkowska G, Goldman-Rakic PS. Elevated neuronal density in prefrontal area 46 in brains from schizophrenic patients: application of a three-dimensional, stereologic counting method. *J Comp Neurol*. 1998;392(3):402-412.
64. Glantz LA, Lewis DA. Decreased Dendritic Spine Density on Prefrontal Cortical Pyramidal Neurons in Schizophrenia. *Arch Gen Psychiatry*. 2000;57(1):65. doi:10.1001/archpsyc.57.1.65
65. Wang Q, Cheung C, Deng W, et al. White-matter microstructure in previously drug-naive patients with schizophrenia after 6 weeks of treatment. *Psychol Med*. 2013;43(11):2301-2309. doi:10.1017/S0033291713000238
66. Okugawa G, Nobuhara K, Takase K, Saito Y, Yoshimura M, Kinoshita T. Olanzapine Increases Grey and White Matter Volumes in the Caudate Nucleus of Patients with Schizophrenia. *Neuropsychobiology*. 2007;55(1):43-46. doi:10.1159/000103575
67. Orr JM, Paschall CJ, Banich MT. Recreational marijuana use impacts white matter integrity and subcortical (but not cortical) morphometry. *Neuroimage Clin*. 2016;12:47-56. doi:10.1016/j.nicl.2016.06.006
68. Ringen PA, Lagerberg TV, Birkenæs AB, et al. Differences in prevalence and patterns of substance use in schizophrenia and bipolar disorder. *Psychol Med*. 2008;38(9):1241-1249. doi:10.1017/S003329170700236X
69. Lin TH, Sun P, Hallman M, et al. Noninvasive Quantification of Axonal Loss in the Presence of Tissue Swelling in Traumatic Spinal Cord Injury Mice. *J Neurotrauma*. 2019;36(15):2308-2315. doi:10.1089/neu.2018.6016
70. George A, Sun P, Cross AH, Wang X, Perez-Torres C, Song SK. Histological validation of diffusion basis spectrum imaging using autopsied multiple sclerosis brain specimen. In: *International Society for Magnetic Resonance in Medicine*. 2017. Accessed February 11, 2024. https://cds.ismrm.org/protected/17MProceedings/PDFfiles/2557.html

FIGURE LEGENDS:

Figure 1: Schematic demonstration of Diffusion Basis Spectrum Imaging (DBSI). A data-driven multipole tensor model is employed by DBSI to model the white matter pathophysiology. Based on the diffusion signatures, DBSI can separate various sub-voxel compartments within the imaging voxel to generate pathologically and physiologically specific imaging biomarkers such as cellular diffusion fraction, axonal water fraction, fiber specific axial and radial diffusivities. In addition, the method can estimate axonal fiber fraction which correlates with axonal fiber density.

Figure 2: TBSS results of DTI-derived fractional anisotropy (FA), axial diffusivity (AD), and radial diffusivity (RD). Red-yellow overlay represents statistically significant difference in FA (Panel A and Panel B), AD (Panel C &D), and RD (Panel E & F) in schizophrenia and bipolar disorder group relative to normal control group ($p < 0.05$, FWER correction by TFCE). To aid visualization, regions showing changes in DTI metric are dilated using 3x3x1 kernel in FSL. Results are shown overlaid on the MNI 152-T1 1mm template and the mean FA skeleton (Blue).

Figure 3. TBSS results of cellular diffusion fraction in healthy control, schizophrenia, and bipolar disorder participants. Red-yellow overlay represents regions with statistically significant changes in cellularity ratio in schizophrenia and bipolar disorder patients (Panel A & B respectively) compared to control subjects ($p < 0.05$, FWER correction by TFCE). To aid visualization, regions showing increased cellularity ratio are dilated using 3x3x1 kernel in FSL. Results are shown overlaid on the MNI 152-T1 1mm template and the mean FA skeleton (Blue).

Figure 4. **TBSS results of axonal fiber fraction in healthy control, schizophrenia, and bipolar disorder participants.** Red-yellow overlay represents statistically significant changes in neuronal density (fiber ratio) in schizophrenia and bipolar disorder subjects (Panel A & B) relative to controls ($p < 0.05$, FWER correction by TFCE). To aid visualization, regions showing decreased fiber1 ratio are

dilated using 3x3x1 kernel in FSL. Results are shown overlaid on the MNI 152-T1 1mm template and the mean FA skeleton (Blue).

Figure 5. TBSS results of DBSI-derived extra-axonal water in healthy control, schizophrenia, and bipolar disorder participants. Red-yellow overlay represents a statistically significantly increased extra-axonal water in schizophrenia and bipolar disorder patients (Panel A & B respectively) relative to controls ($p < 0.05$, FWER correction by TFCE). To aid visualization, regions showing increased fiber23 ratio are dilated using 3x3x1 kernel in FSL. Results are shown overlaid on the MNI 152-T1 1mm template and the mean FA skeleton (Blue).

Figure 6. TBSS results of DBSI-derived axial and radial diffusivity in healthy control, schizophrenia, and bipolar disorder participants. Red-yellow overlay represents statistically significant difference in fiber axial diffusivity (Panel A & B) and fiber radial diffusivity (Panel C & D) in schizophrenia and bipolar disorder group (respectively) relative to controls ($p < 0.05$, FWER correction by TFCE). To aid visualization, regions showing increased radial diffusivity are dilated using 3x3x1 kernel in FSL. Results are shown overlaid on the MNI 152-T1 1mm template and the mean FA skeleton (Blue).

Figure 7. Relationship between WERCAP-Psychosis symptom score and DBSI measures in schizophrenia (in red), in control (in black), and in combined group (in green). Scatterplots showing significant correlation between WERCAP-Psychosis score and DBSI measures – (A) Cellular diffusion fraction, (B) DBSI-derived radial diffusivity, (C) Fiber density, and (D) extra-axonal water. Shaded region surrounding regression lines shows 95% confidence interval.

Figure 8. The associations between WERCAP-Affectivity symptom score and DBSI measures in schizophrenia (in red), in control (in black), and in combined group (in green). Scatterplots showing significant correlation between WERCAP-Affectivity score and DBSI measures – (A) Cellular diffusion fraction, (B) DBSI-derived radial diffusivity, (C) Fiber density, and (D) extra-axonal water. Shaded region surrounding regression lines shows 95% confidence interval.

Table 1. Baseline demographics and medication history across participant groups.

Characteristic	**CON**, N = 27[1]	**BP**, N = 21[1]	**SCZ**, N = 21[1]	**p-value**[2]
Age	25.56 (3.3)	27.00 (3.6)	26.71 (4.1)	0.3
Gender				0.076
Female	16 (59.3%)	17 (81.0%)	10 (47.6%)	
Male	11 (40.7%)	4 (19.0%)	11 (52.4%)	
BMI	26.47 (6.6)	29.96 (7.4)	29.69 (7.8)	0.15
BMI group				
Underweight	1 (3.7%)	1 (4.8%)	1 (4.8%)	
Healthy	12 (44.4%)	4 (19.0%)	5 (23.8%)	
Overweight	7 (25.9%)	7 (33.3%)	6 (28.6%)	
Obese	7 (25.9%)	9 (42.9%)	9 (42.9%)	
Anti-psychotic medications				
Typical neuroleptics	0	0	3 (14.3%)	
Atypical neuroleptics	0	5 (23.8%)	10 (47.6%)	
Mood stabilizers				
Lithium	0	0	2 (9.5%)	
Anti-convulsant	0	6 (28.6%)	2 (9.5%)	
Both	0	2 (9.5%)	0	
Anti-depressants				
SSRI/SNRI	1 (3.7%)	1 (4.8%)	6 (28.6%)	
Atypical	0	2 (9.5%)	2 (9.5%)	
Both	0	0	1 (4.8%)	
Other/No medications				
Other[3]	0	3 (14.3%)	3 (14.3%)	
None[4]	26 (96.3%)	10 (47.6%)	7 (33.3%)	

[1] Mean (SD); N (%)
[2] Kruskal-Wallis rank sum test; Pearson's Chi-squared test
[3] Participants with active benzodiazepines, anticholinergics, and beta-blockers.
[4] Participants with no active medication at all during the time of assessment.

Table 2: Summary of changes in DTI and DBSI measures across WM tracts and disease group (Health Control=HC, Schizophrenia=SCZ, Bipolar disorder=BPD). ↑ denotes significant increase. ↓ denotes significant decrease and – denotes no statistically significant change. R denotes significant change in right hemisphere only, L denotes significant change in left hemisphere only, and arrow without R or L denotes change in both hemisphere.

Diffusion parameter	DTI FA		DTI RD		DTI AD		Cellular diffusion fraction		Axonal fiber fraction		Extra-axonal water fraction		Fiber radial diffusivity		Fiber axial diffusivity	
Group comparison / **WM tracts**	HC vs. SCZ	HC vs. BPD	HC vs. SCZ	HC vs. BPD	HC vs. SCZ	HC vs. BPD	HC vs. SCZ	HC vs. BPD	HC vs. SCZ	HC vs. BPD	HC vs. SCZ	HC vs. BPD	HC vs. SCZ	HC vs. BPD	HC vs. SCZ	HC vs. BPD
Anterior thalamic radiation	↓	↓ (L)	↑	--	--	--	↑	--	↓	--	↑	↑	↑	↑	--	--
Cingulum (cingulate gyrus)	↓	↓	↑	--	--	--	↑	--	↓	--	↑	↑	↑	↑	--	--
Cingulum (hippocampus)	↓	--	↑	--	--	--	↑	--	↓	--	↑	↑	↑	↑	--	--
Corticospinal tract	↓	--	↑	--	--	--	↑	--	↓	--	↑	↑	↑	↑	--	--
Forceps major	↓	--	↑	--	--	--	↑	--	↓	--	↑	↑	↑	↑	--	--
Forceps minor	↓	↓	--	--	--	--	↑	--	↓	--	↑	↑	↑	↑	--	--
Inferior fronto-occipital fasciculus	↓	↓ (L)	↑	--	--	--	↑	--	↓	--	↑	↑	↑	↑	--	--
Inferior longitudinal fasciculus	↓	--	↑	--	--	--	↑	--	↓	--	↑	↑	↑	↑ (R)	--	--
Superior longitudinal fasciculus (temporal part)	↓	--	↑	--	--	--	↑	--	↓	--	↑	↑	↑	↑	--	--
Superior longitudinal fasciculus	↓	--	↑	--	--	--	↑	--	↓	--	↑	↑	↑	↑	--	--
Uncinate fasciculus	↓	↓ (L)	--	--	--	--	↑	--	↓	--	↑	↑	↑	↑ (L)	--	--

Figure 1: Schematic demonstration of Diffusion Basis Spectrum Imaging (DBSI).

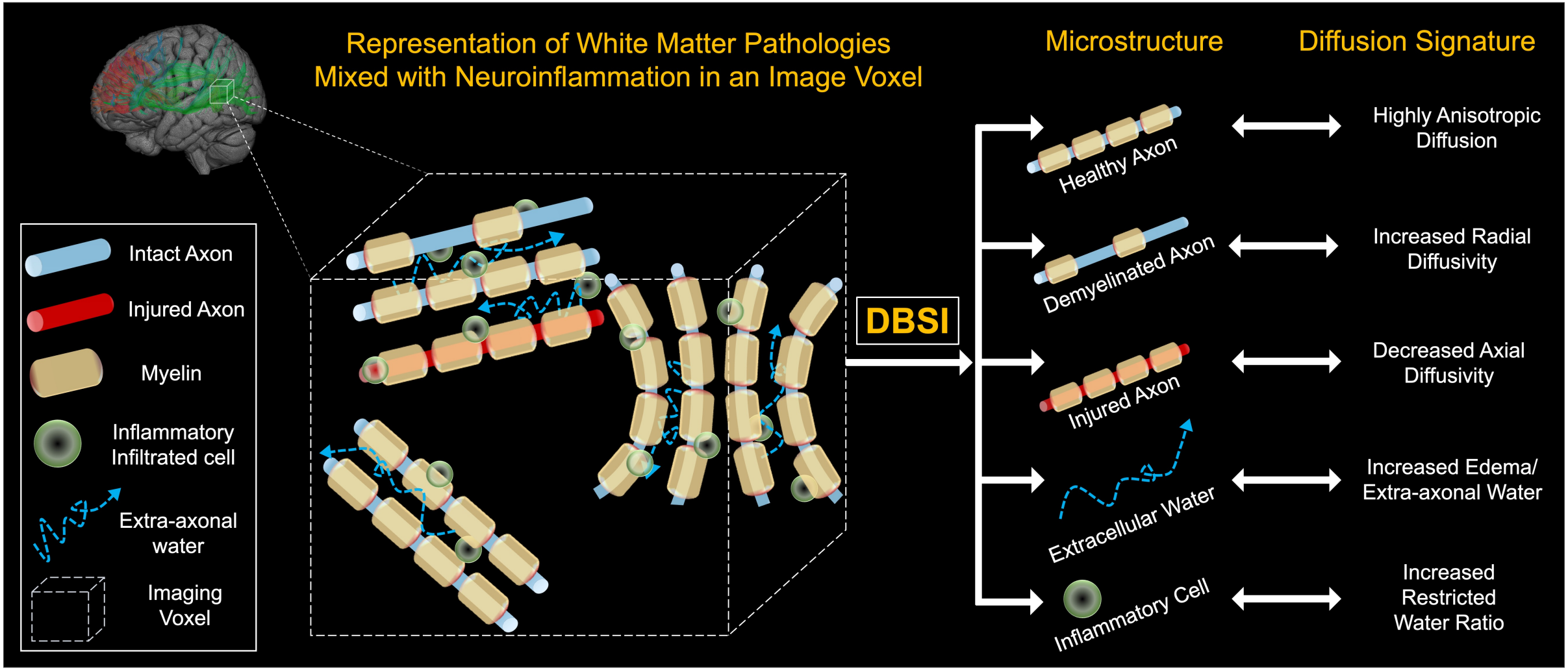

Figure 2: TBSS results of DTI-derived fractional anisotropy (FA), axial diffusivity (AD), and radial diffusivity (RD).

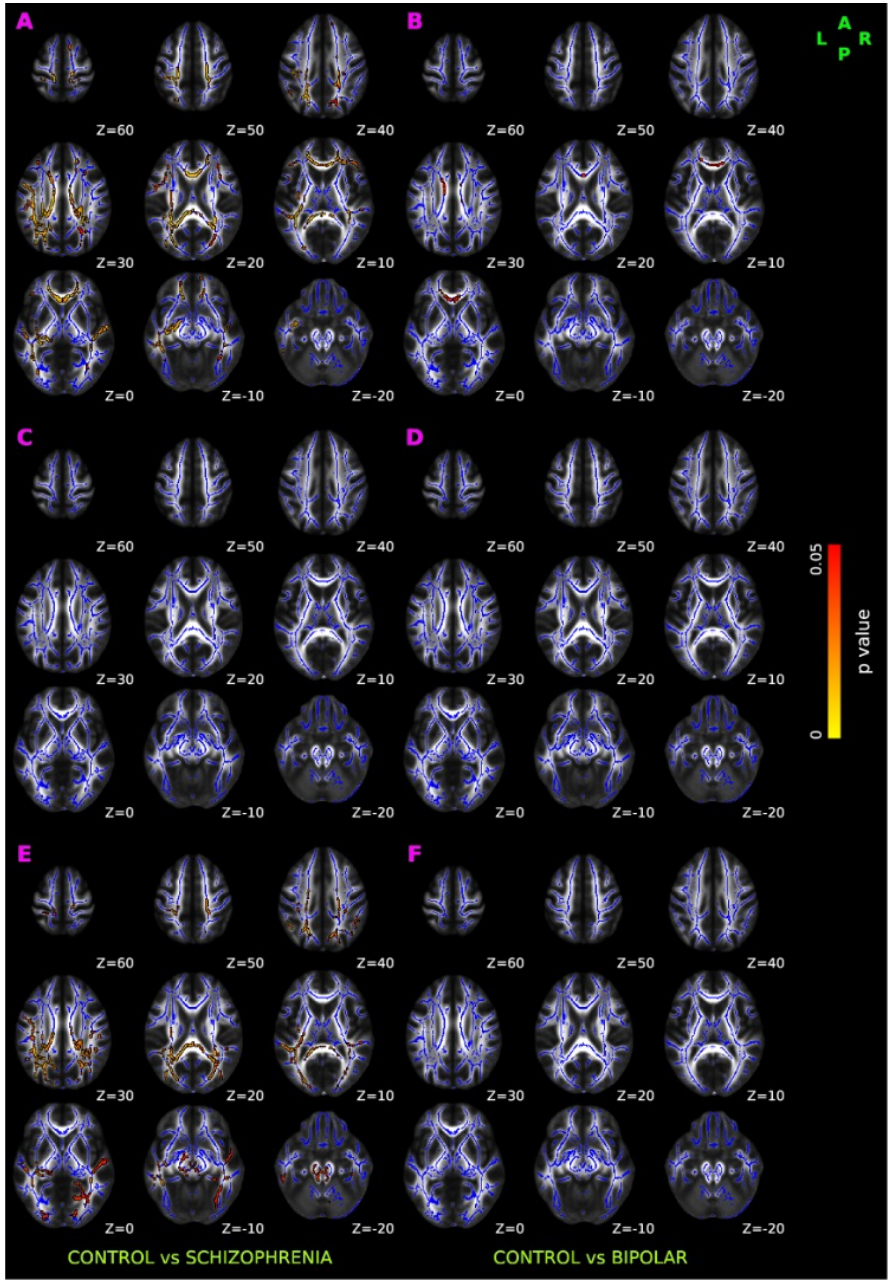

Figure 3. TBSS results of DBSI-derived cellular diffusion fraction in healthy control, schizophrenia and bipolar disorder participants.

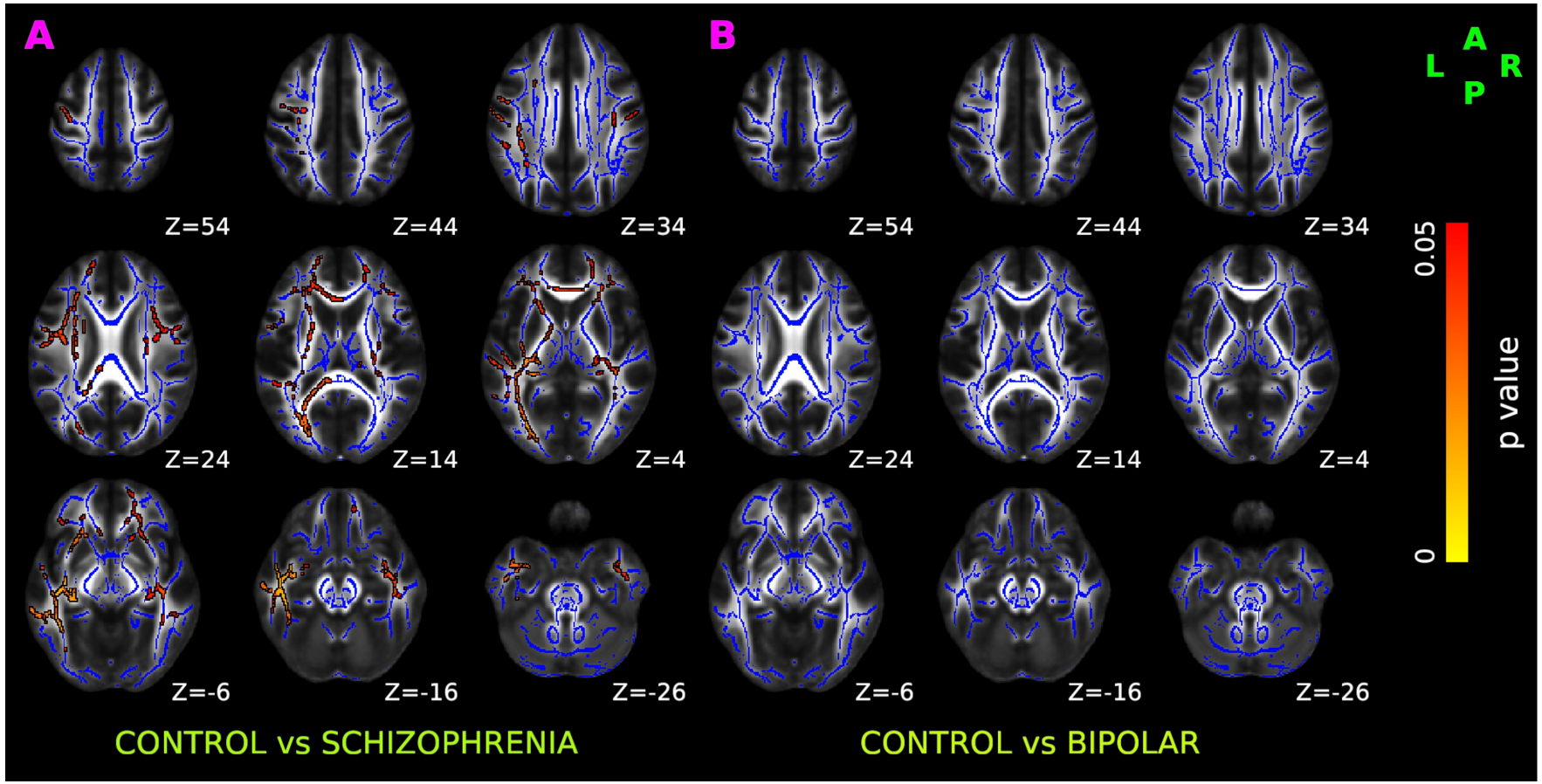

Figure 4. TBSS results of DBSI-derived axonal fiber fraction measure in healthy control, schizophrenia and bipolar disorder participants.

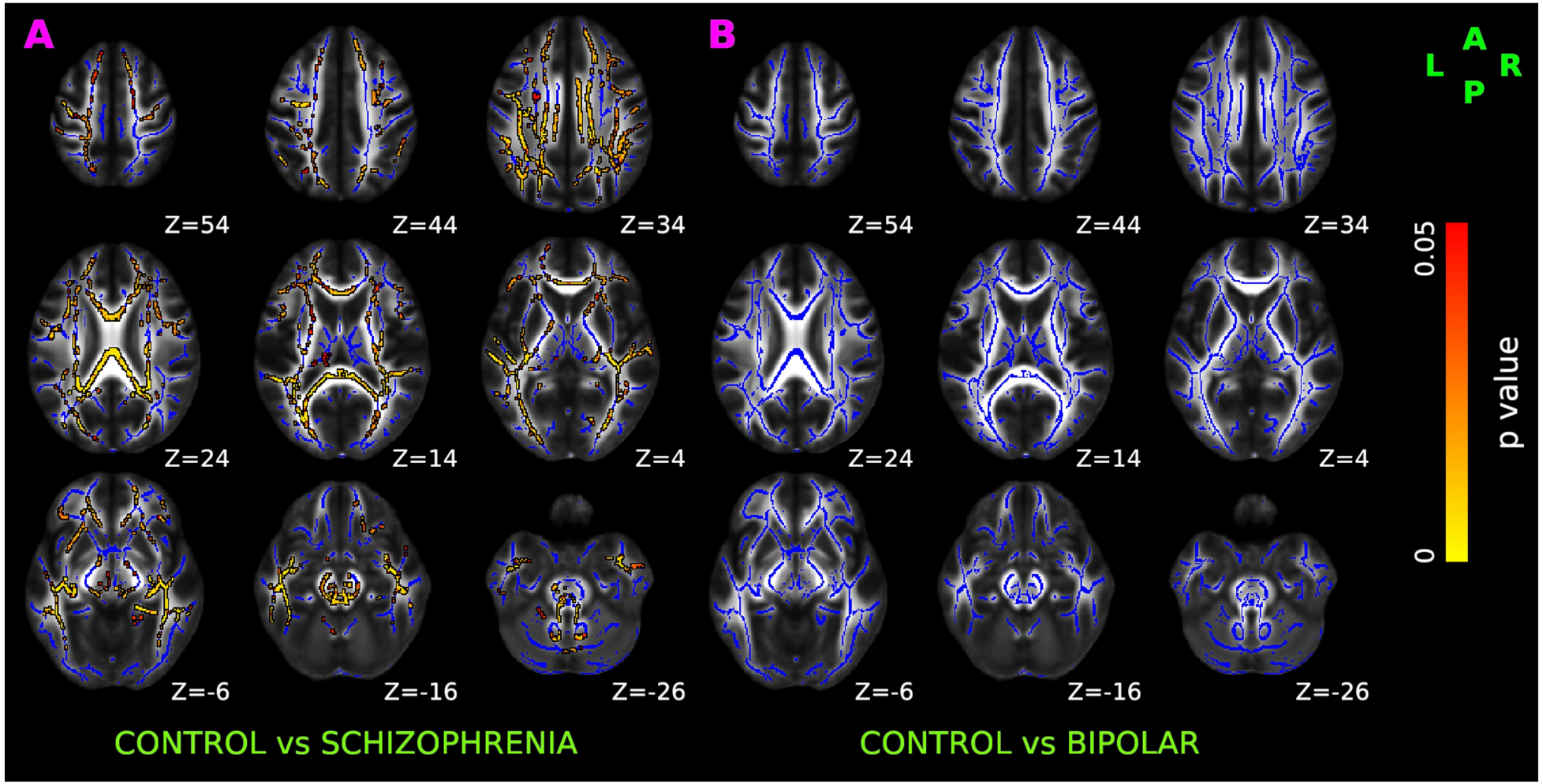

Figure 5. TBSS results of DBSI-derived extra-axonal water fraction in healthy control, schizophrenia and bipolar disorder participants.

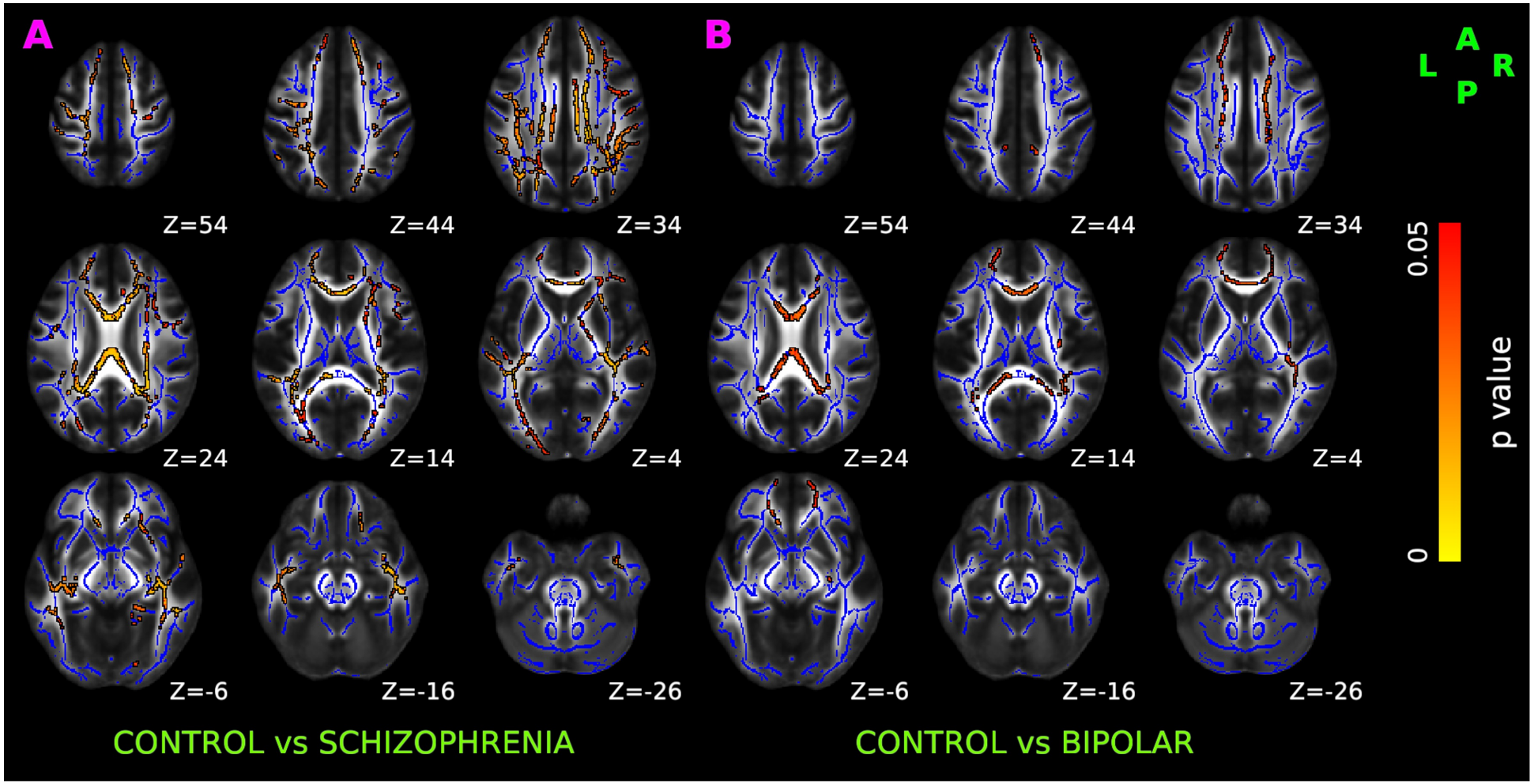

Figure 6. TBSS results of DBSI-derived fiber axial and radial diffusivity in healthy control, schizophrenia and bipolar disorder participants.

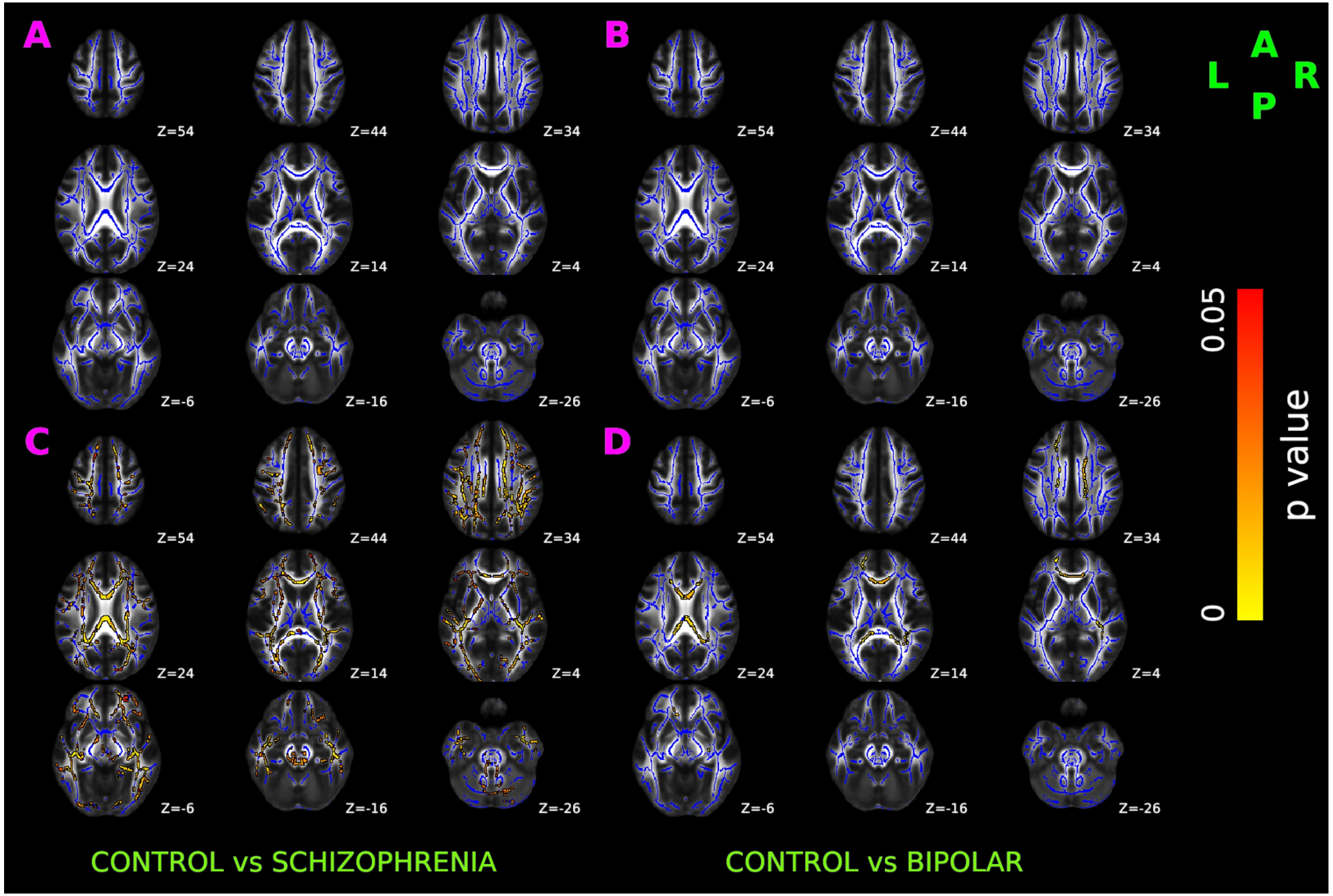

Figure 7. Relationship between WERCAP-Psychosis symptom score and DBSI measures in schizophrenia (in red), in control (in black), and in combined group (in green).

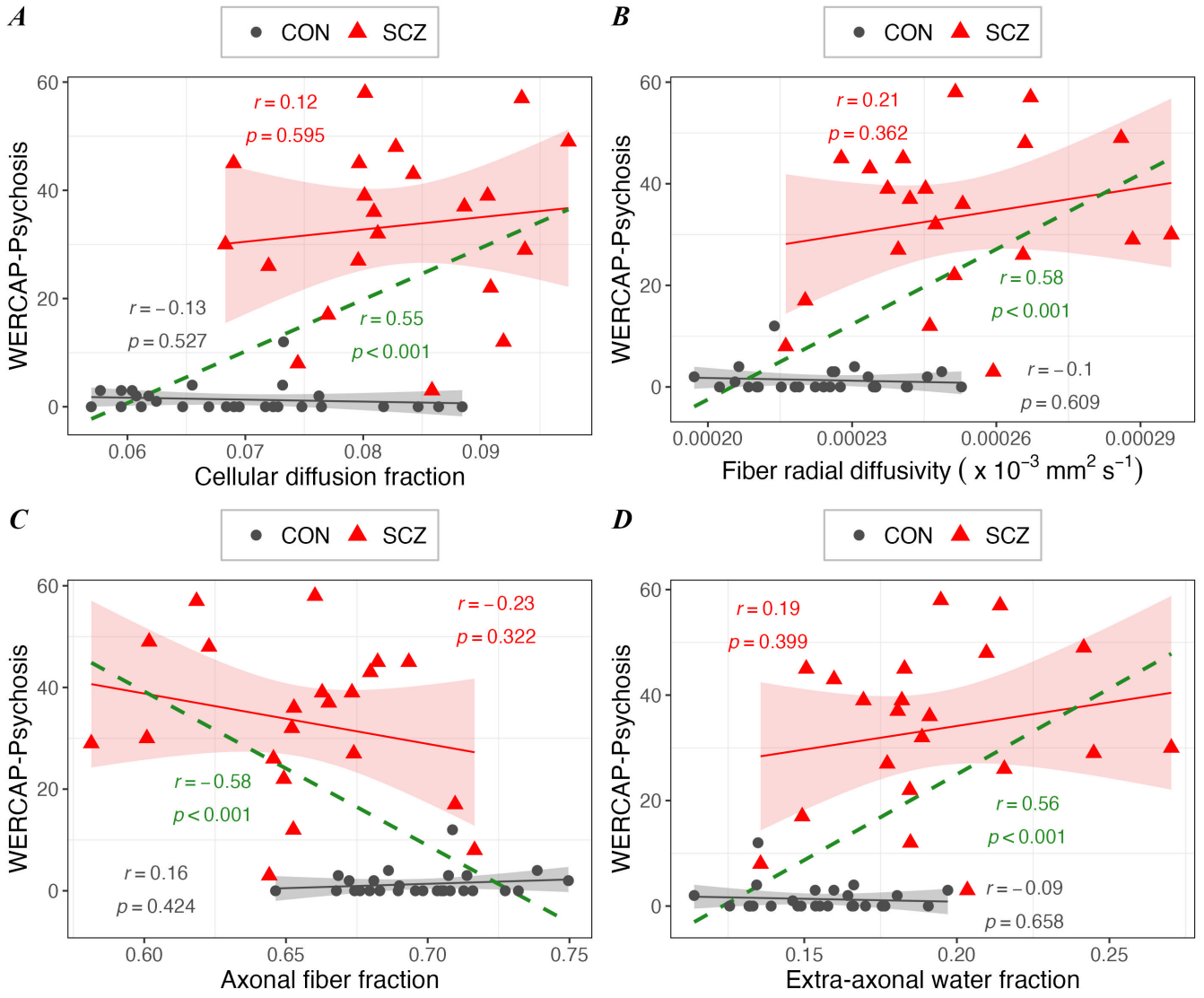

Figure 8. The associations between WERCAP-Affectivity symptom score and DBSI measures in schizophrenia (in red), in control (in black), and in combined group (in green).